# Technical Notes

*TECHNICAL NOTES are short manuscripts describing new developments or important results of a preliminary nature. These Notes cannot exceed 6 manuscript pages and 3 figures; a page of text may be substituted for a figure and vice versa. After informal review by the editors, they may be published within a few months of the date of receipt. Style requirements are the same as for regular contributions (see inside back cover).*

## Extensions of Dual-Plate Holographic Interferometry

B. W. Hannah* and W. L. King Jr.†
*Naval Surface Weapons Center, White Oak Laboratory, Silver Spring, Md.*

A DUAL-plate holographic interferometer system of unique capability has been reported.[1] The basic scheme is an extension of the system enumerated in Refs. 2 and 3. These systems differ from the conventional holographic interferometers in that they store the reference and scene wave-fronts on separate holograms, and the interferometric image is not created until reconstruction.

The dual-plate approach has several advantages over the traditional single plate dual-exposure method. They include insensitivity to mechanical vibration, availability of Schlieren and shadowgraph images from the same holograms generating the interferograms, and the ability to arbitrarily position the interference fringes during reconstruction. It will be demonstrated that the ability to arbitrarily maneuver fringes during reconstruction is essential to the quantitative practical application of interferometry.

### Instrumentation

The basic instrumentation system and components have been described in Ref. 1. One critical component, essential to the successful application of the method, is the dual-plate micropositioner used to position the dual holograms during reconstruction. The original micropositioner developed by Havener[2,3] and improved by Hannah and Havener[1] suffered from several deficiences, the most serious being the mechanical coupling between the various degrees of hologram mechanical movement.

As a result, an improved micropositioner has been built. Its design allows the holographic plates to be mounted directly into the micropositioner and provides six degrees of uncoupled mechanical motion. The detailed design of this micropositioner will be published in the near future.

### Quantitative Data Reduction

One of the main problems in quantitative production applications of interferometry is the basic lack of continuous data in conventional interferometric images. In any given image, only a limited number of fringes cross any line along which quantitative data are desired. The ideal situation would be the generation of a data curve giving fringe shift as a continuous function of position in the flow, but the number of data points in any single image precludes this possibility.

Presented at the AIAA 9th Aerodynamic Testing Conference, Arlington, Texas, June 7-9, 1976; submitted July 12, 1976; revision received Feb. 7, 1977.

Index categories: Research Facilities and Instrumentation; Supersonic and Hypersonic Flow

*Aerospace Engineer. Member AIAA.

†Photographic Engineer.

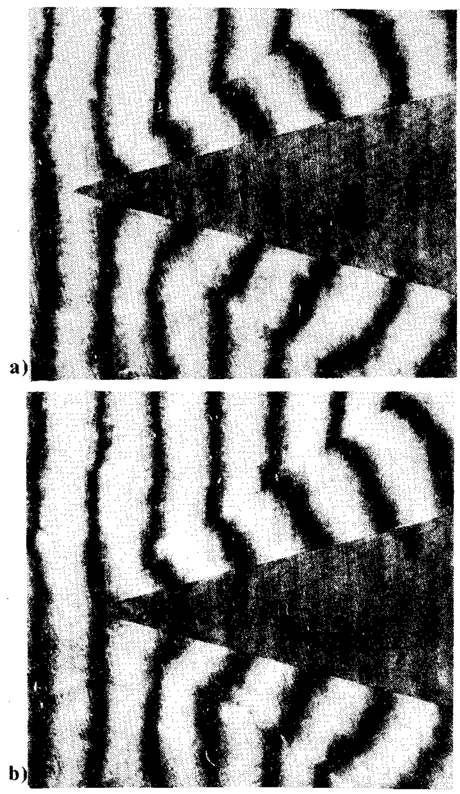


**Fig. 1 Single-image fringe shift.**

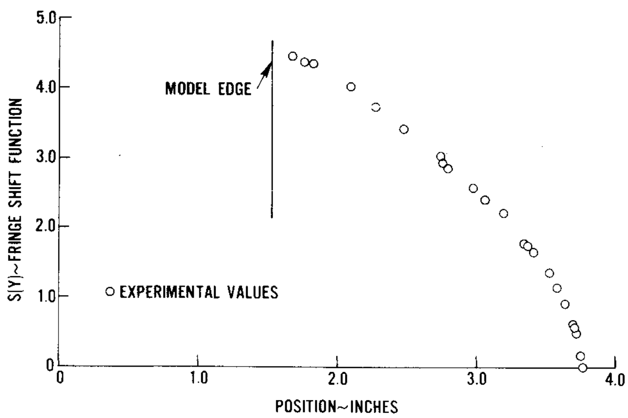


**Fig. 2 Fringe shift data.**

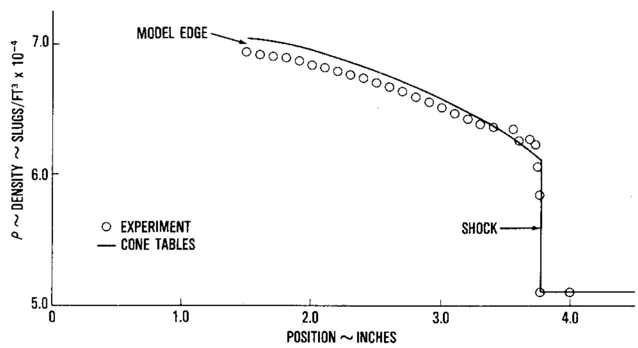


**Fig. 3 Quantitative data comparison.**

a)
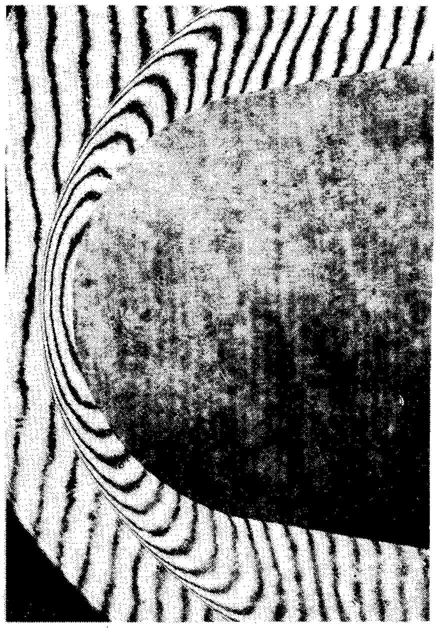

b)


**Fig. 4 Flowfield without/with surface blowing.**

a)
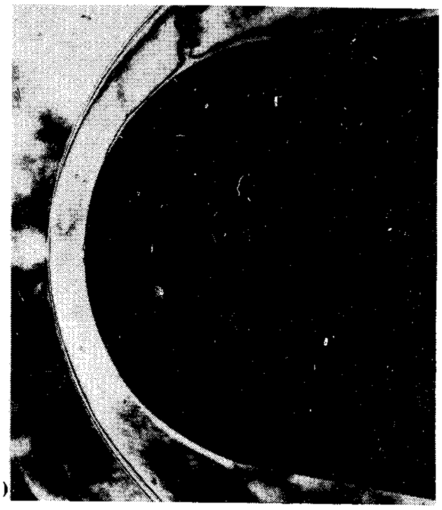

b)
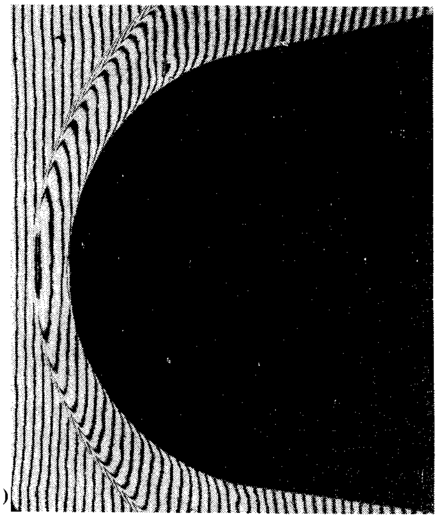

**Fig.5 Infinite/finite interferogram of flowfield change due to blowing.**

In the classic analysis employing the derivative of the fringe shift function, gross errors would originate from a function defined by only a few data points. Even for methods that overcome the use of derivatives by transformation of variables or in three-dimensional inversion techniques, the accuracy is directly related to the accuracy of the measured fringe shift function.

As an offshoot of a previously reported effort,[1] a method has been devised to overcome this problem. By micromanipulation of the dual holographic plates it is possible to maneuver the fringes in a controlled fashion for any given test image. Figure 1 shows the fringe pattern for a single scene, which has been shifted by approximately one half of a nominal fringe spacing.

With the ability to laterally shift fringes during the reconstruction, a fringe may be positioned such that it crosses the line of interest at any desired location. Figure 2 shows the raw data for the conical flowfield under consideration where five fringe patterns, constituting a total freestream shift of one fringe space, were used. This method provided 23 data points for this test case as opposed to five for any one image. For the generation of quasicontinuous data, fringe shifts of the order of 10% of the nominal fringe spacing are needed. This represents a linear micrometer movement of 0.0001 inch (angular rotation of four arc sec), therefore making the use of piezoelectric micrometers essential to the method.

Figure 3 shows a comparison between experimental data employing this method and theory for an inviscid axisymmetric supersonic conical flowfield. It should be noted that this measurement includes quantitative determination of the shock strength as well as the mild inviscid compression to the cone surface. Additional quantitative comparisons can be found in Ref. 3.

## Application to Porous Model Blowing

After the initial tests of the interferometry system, it was desired to determine the susceptibility of the total system to vibration. The system was therefore set up as a piggyback on an existing test of a highly blunted (nose radius of 2.25 in.) roughened porous model with distributed surface blowing.

Figure 4a shows a finite fringe dual-plate interferogram of this model. Flow conditions of $M=6.0$, $P_0=250$ psia, and $T_0=660°$F were maintained during the run. The flow rate through the porous surface was adjusted to equal the stagnation pressure at the nose, thereby minimizing the effects of gas injection on the flowfield. Figure 4b represents the same freestream conditions with the injection system providing maximum flow rate. A marked difference in the surface flowfield can be seen, due to surface blowing, and could be used to generate flowfield density profile. Note that in Fig. 4 the reference hologram was made with model out, tunnel off, and the scene hologram was made with model in and tunnel on.

During this test series, runs were also made to determine if an interferogram could be made that reflected only the change in flowfield due to gas injection. This would facilitate both qualitative and quantitative determination of the effects of surface blowing. For these tests, the reference hologram was made with tunnel on, model in, but no surface blowing. Figure 5 shows infinite and finite interferograms of this case and clearly demonstrates that the effect of the mean flowfield, common to both cases, can be completely negated.

The asymmetry on the upper nose corner was traced to a slight leak in the porous material joint at this location. The effect of this leak on the asymmetry of the shock can be seen in Fig. 5b (upper right). It is seen that this test series demonstrates both system insensitivity to vibration and wide versatility in realistic applications.

## Conclusions

Advances in technique and several new applications have been enumerated. These advances are seen as part of a continuing program to develop an automated production-type holographic interferometry system capable of three-dimensional quantitative flow-field measurement. Future work will be directed toward completion of the computerized reader scanner system described in Ref. 1.

## Acknowledgment

This work was supported by the Naval Air Systems Command (AIR-310) under AIRTASK A310-3100/0041.

## References

[1]Hannah, B. W. and Havener, A. G., "Applications of Automated Holographic Interferometry," presented at *International Congress on Instrumentation in Aerospace Simulation Facilities,* Ottawa, Canada, Sept. 1975, pp. 237-246.

[2]Havener, A. G. and Radley, R. J., "Supersonic Wind Tunnel Investigation Using Pulsed Laser Holography," Rept. 73-0148, Oct 1973.

[3]Radley, R. J. Jr., and Havener, A. G., "The Application of Dual Hologram Interferometry to Wind Tunnel Testing," *AIAA Journal,* Vol. 11, Sept. 1973, pp. 1332-1333.

# Prediction of Turbulent Boundary Layers on Cones at Incidence

Kalle Kaups* and Tuncer Cebeci†
*Douglas Aircraft Company, Long Beach, Calif.*

## Introduction

IN this Note, we discuss the prediction of turbulent boundary layers on circular cones at incidence by an efficient numerical method. The method employs the eddy-viscosity concept to model the Reynolds shear stress terms and has been previously used to compute two-dimensional boundary layers[1] and recently three-dimensional boundary layers.[2-4] Our method differs from the others[5,6] in that it utilizes a recent suggestion of Bradshaw et al.[7]; rather than using the $y/\sqrt{x}$-similarity variable to reduce the governing equations to a similarity form as is done for laminar flows, we use the $y/x$-similarity variable for turbulent flows. Our study shows that this scaling provides better agreement with experiment than the "old" procedure.

Received Sept. 16, 1976; revision received Feb. 7, 1977.

Index categories: Boundary Layers and Convective Heat Transfer—Turbulent.

*Senior Engineer/Scientist. Member AIAA.

†Chief Aerodynamics Engineer, Research. Member AIAA.

## Governing Equations

The governing boundary-layer equations for compressible laminar and turbulent flows on a conical surface are given by the following equations:

Continuity:

$$\frac{\partial}{\partial x}(x\rho u)+\frac{\partial}{\partial \theta}(\rho w)+\frac{\partial}{\partial y}(x\overline{\rho v})=0 \tag{1}$$

$x$-Momentum:

$$\rho u\frac{\partial u}{\partial x}+\rho\frac{w}{x}\frac{\partial u}{\partial \theta}+\overline{\rho v}\frac{\partial u}{\partial y}-\rho\frac{w^2}{x}=\frac{\partial}{\partial y}\left(\mu\frac{\partial u}{\partial y}-\rho\overline{u'v'}\right) \tag{2}$$

$\theta$-Momentum

$$\rho u\frac{\partial w}{\partial x}+\rho\frac{w}{x}\frac{\partial w}{\partial \theta}+\overline{\rho v}\frac{\partial w}{\partial y}+\rho\frac{uw}{x}=-\frac{1}{x}\frac{\mathrm{d}p}{\mathrm{d}\theta}$$
$$+\frac{\partial}{\partial y}\left(\mu\frac{\partial w}{\partial y}-\rho\overline{w'v'}\right) \tag{3}$$

Energy

$$\rho u\frac{\partial H}{\partial x}+\rho\frac{w}{x}\frac{\partial H}{\partial \theta}+\overline{\rho v}\frac{\partial H}{\partial y}=\frac{\partial}{\partial y}\left[\frac{\mu}{Pr}\frac{\partial H}{\partial y}\right.$$
$$\left.+\mu\left(1-\frac{1}{Pr}\right)\frac{\partial}{\partial y}\left(\frac{u^2+w^2}{2}\right)-\rho\overline{v'H'}\right] \tag{4}$$

Here $\overline{\rho v}=\rho v+\overline{\rho' v'}$; $\theta$ denotes the polar coordinate in the developed plane; $x$ the coordinate along the generators; and $y$ the coordinate normal to the surface; with $w$, $u$, $v$ the velocities in the $\theta$, $x$, and $y$ directions.

At the windward stagnation line, $\theta=0$, the cross-flow momentum equation is singular since $w\equiv 0$. Taking into account the symmetry conditions and differentiating Eq. (3) with respect to $\theta$, we can write it as

$$\rho u\frac{\partial w_\theta}{\partial x}+\rho\frac{w_\theta^2}{x}+\overline{\rho v}\frac{\partial w_\theta}{\partial y}+\rho\frac{uw_\theta}{x}=-\frac{1}{x}\frac{\mathrm{d}^2p}{\mathrm{d}\theta^2}$$
$$+\frac{\partial}{\partial y}\left[\mu\frac{\partial w_\theta}{\partial y}-\rho(\overline{w'v'})_\theta\right] \tag{5}$$

Noting that $w=0$, Eqs. (1, 2, and 4) can be simplified and written as

$$\frac{\partial}{\partial x}(x\rho u)+\rho w_\theta+\frac{\partial}{\partial y}(x\overline{\rho v})=0 \tag{6}$$

$$\rho u\frac{\partial u}{\partial x}+\overline{\rho v}\frac{\partial u}{\partial y}=\frac{\partial}{\partial y}\left(\mu\frac{\partial u}{\partial y}-\rho\overline{u'v'}\right) \tag{7}$$

$$\rho u\frac{\partial H}{\partial x}+\overline{\rho v}\frac{\partial H}{\partial y}=\frac{\partial}{\partial y}\left[\frac{\mu}{Pr}\frac{\partial H}{\partial y}+\mu\left(1-\frac{1}{Pr}\right)\frac{\partial}{\partial y}\left(\frac{u^2}{2}\right)-\rho\overline{v'H'}\right] \tag{8}$$

where $w_\theta=\partial w/\partial\theta$.